International Journal of Modern Physics B
Vol. 33, Nos. 1–3 (2019) 1940038 (10 pages)

DOI: 10.1142/S0217979219400381

Evaluate welding residual of 6082-T6 aluminum alloy welded plate by using ultrasonic method

Zhongyin Zhu*, Guoqing Gou*,§, Zhiyi Zhang†,
Chuanping Ma* and Wei Gao‡

**Key Laboratory of Advanced Technologies of Materials, Ministry of Education China, Southwest Jiaotong University, Chengdu 610031, P. R. China*

†CRRC Qingdao Sifang Locomotive Co. Ltd, Qingdao 266550, P. R. China

‡Department of Chemical and Materials Engineering, The University of Auckland, PB 92019, Auckland 1142, New Zealand

§gouguoqing1001@163.com

Received 1 July 2018
Revised 30 August 2018
Accepted 15 September 2018
Published 3 January 2019

The residual stress beneath the surface is crucial to the safety of the structures. Neutron Diffraction and Hole-drilling are the two methods being used to measure the inner residual stress. Longitudinal Critically Refracted (LCR) wave transmission that is propagated parallel to surface also can be used for measuring residual stress, but measurements are within an effective depth and need to be further studied. In this paper, the parameters of K are separately tested in WZ, HAZ and BM zone. The welding process of 6082-T6 aluminum alloy welded joints is simulated in SYSWELD, the finite element model has been verified by the X-ray diffraction method. The residual stress value calculated by SYSWELD and the values obtained from the ultrasonic measurement show a good agreement. It is demonstrated that the residual stress of 6082-T6 aluminum alloy welded plate can be evaluated by using the ultrasonic method.

Keywords: Longitudinal critically refracted wave; welding residual stress; 6082-T6; finite element.

PACS number: 81.20.Vj

1. Introduction

6082 aluminum alloy is widely used in the production of high-speed train body because of its high strength, due to its large linear expansion coefficient, which

§Corresponding author.

resulted in the large volume shrinkage then the residuals stress in welding components was higher. Residual stress affects the performance of high-speed strain on service, such as fatigue life, stress corrosion resistance, brittleness fracture and the stability of the size. Efficient and reliable measuring residual stress is one of the most important challenges to the safety of high-speed train.

In the past years, various nondestructive techniques have been developed to measure the residual stress, the strain gauge method,[1] X-ray diffraction,[2–4] and neutron diffraction method.[5] Unfortunately, there is no reliable method which gives complete satisfaction in the *in situ* stress monitoring of the welded structures. Material, geometry, surface quality, cost and accuracy of the measurement are some of the parameters that must be taken into account in choosing a proper method. Therefore, the ultrasonic wave stress method is inevitable. The critical refraction longitudinal (L_{CR}) wave method is widely used, which is relies on the variations between the velocity of the ultrasonic wave and the material stress to evaluate the residual stress.[6–8]

The main goal of this research is to carry out a feasibility study for nondestructive stress measurement to evaluate the welding residual stress of 6082-

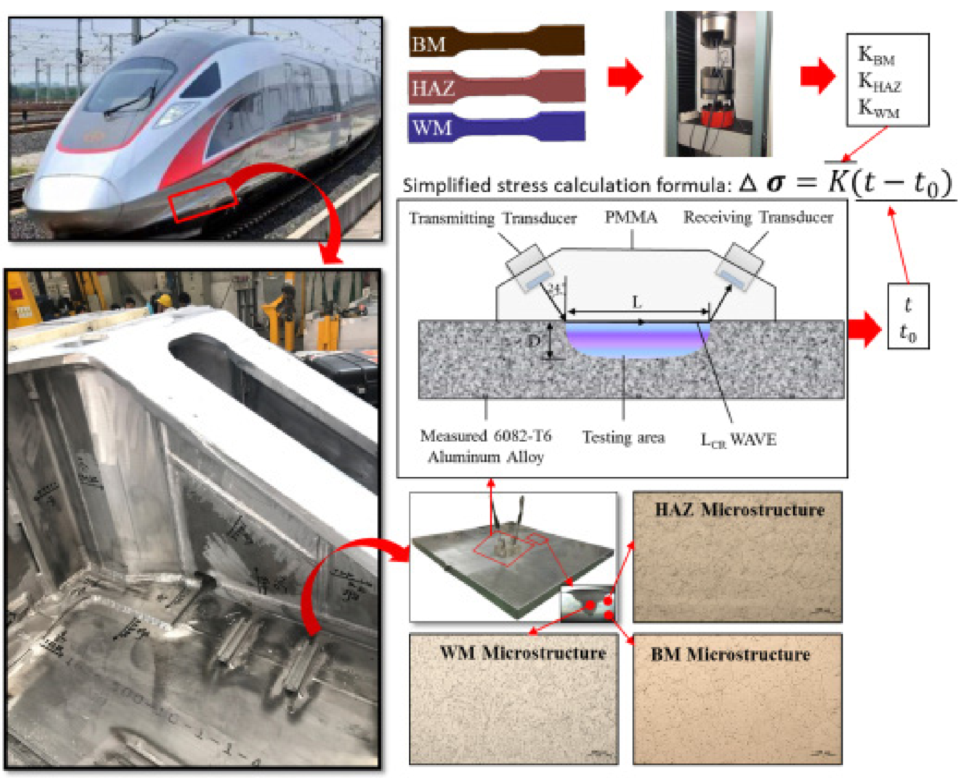

Fig. 1. (Color online) Article framework and research background.

T6aluminum alloy welded joint (Fig. 1). The parameters of K (stress coefficient) are separately tested in weld zone (WZ), heat-affected zone (HAZ), and base metal (BM) zone, then the residual stress is compared with FEM method by Sysweld software calculation.

2. Theoretical Background

2.1. *LCR stress measurement method*

According to Snell's law,[9] when ultrasonic velocity in the second medium is greater than in the first one, the angle of the refracted longitudinal wave increases with the increase of the incidence angle of the longitudinal wave. When the incident angle increases to a certain value, the refracted longitudinal wave travels parallel to member surface. These waves are called longitudinal critically refracted waves, or L_{CR} waves.

The relation between measured travel-time change of L_{CR} wave and the corresponding uniaxial stress derived by Egle and Bray[10] is

$$d\sigma = \frac{EdV_{11}}{V_{11}L_{11}} = \frac{E}{L_{11}t_0}dt, \tag{1}$$

where $d\sigma$ is the stress variation; E is the elasticity modulus; and dt is the variation of time-of-flight (TOF); and t_0 is the time for the wave which travels through a stress-free path in the material being investigated.

By assuming that K represents $E/L_{11}t_0$, Eq. (1) can be simplified to Eq. (2) in which K is called the stress coefficient with the unit of MPa/ns.

$$\Delta\sigma = K\Delta t, \tag{2}$$

where $\Delta\sigma$ is the observed change in applied stress (MPa); Δt is L_{CR} wave time-of-flight varying in the test samples.

2.2. *FE simulation*

In this study, three-dimensional finite element models are developed in Sysweld software. The solution procedure consists of two steps; first, the temperature history and different phase proportions are computed by coupling between heat transfer and phase transformation analyses in order to better approach the actual heat source condition, 3D double ellipsoid heat source model[11] (Fig. 2) was chosen for welding numerical simulation.

In the next step, the mechanical analysis is accomplished which is based on the usual equations of the static equilibrium.The temperature fields computed by the thermal analysis, are used in the mechanical analysis. The FE model of plates is shown in Fig. 3.

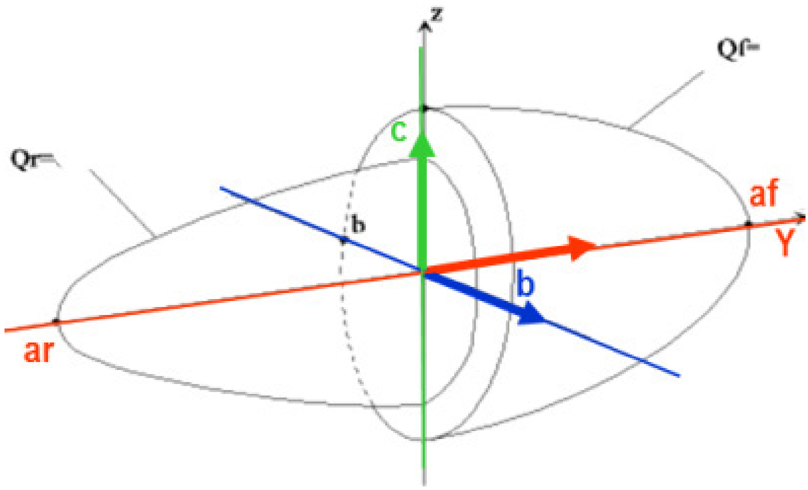

Fig. 2. (Color online) Double ellipsoid heat source model.

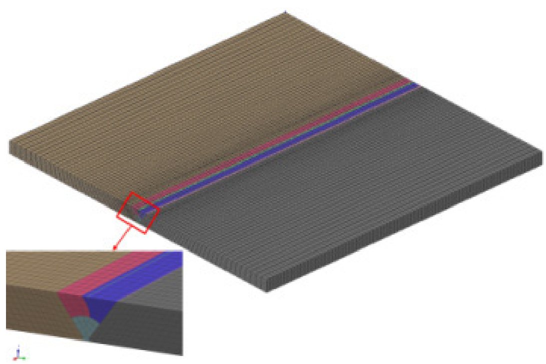

Fig. 3. (Color online) FE model.

3. Material and Measure Systems

3.1. *Materials and welding parameters*

Two 6082 Al alloy plates with the dimension of 300 × 150 × 12 mm under T6 aging condition (solution-treated and naturally aged according to ISO 2107:2007) were used in this study. Joints were processed by the metal inert gas (MIG) technique with a Kemppi arc pulse 450 welding machine. The parameters of the welding process are listed in Table 1.

3.2. *Measurement system*

A measurement system is designed in this study, which includes a total of four components in the system (Fig. 4). Respectively, (1) the core device is used to

Table 1. Welding processing parameters.

Weld No.	Current, A	Voltage, V	Speed, cm/min	Schematic sequence
1	180–200	21	45–55	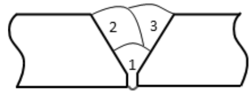
2	210–220	23	40–50	
3	210–220	24	40–50	

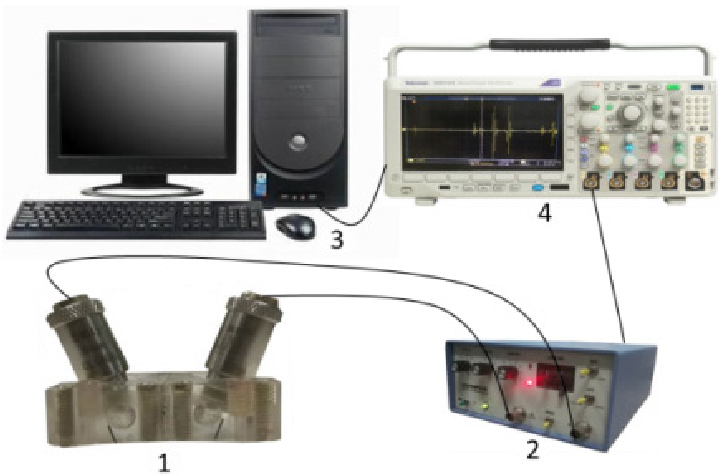

Fig. 4. (Color online) Measurement system.

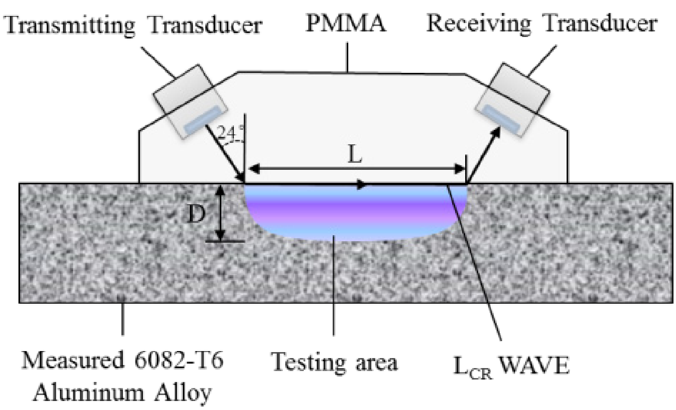

Fig. 5. (Color online) LCR wave testing device.

generate and receive L_{CR} waves. The generated ultrasonic wave propagates from poly methyl methacrylate (PMMA) material to the steel, and then to the receiving probe via PMMA material, we calculated the incidence angle of the longitudinal wave as 24° from Snell's law (Fig. 5), the diameter of all the piezoelectric elements was 6 mm and their nominal frequencies were 5 MHz, the measured depth of the Al samples was about 1.4 mm; (2) a Panametrics 5072PR pulser receiver; (3) a data-processing computer; (4) the oscilloscope with the sampling frequency of 5 GHz (Tektronix company production, MDO3104).

3.3. *Correction of stress coefficient K*

In order to obtain stress coefficient K of different zones, six rectangular tension tests were extracted to determine the stress co efficient K (Fig. 6), two specimens were extracted from the base material (BM) zone, two specimens were extracted from the melted zone (MZ), two specimens were extracted from the parent material and then

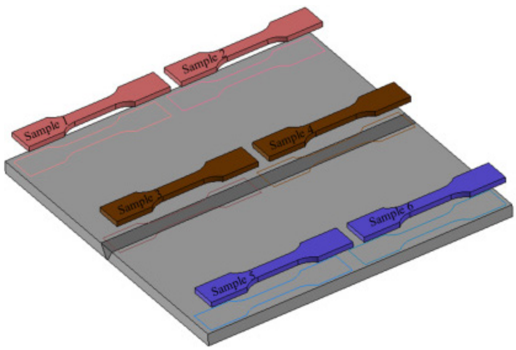

Fig. 6. (Color online) Sample location in each zone.

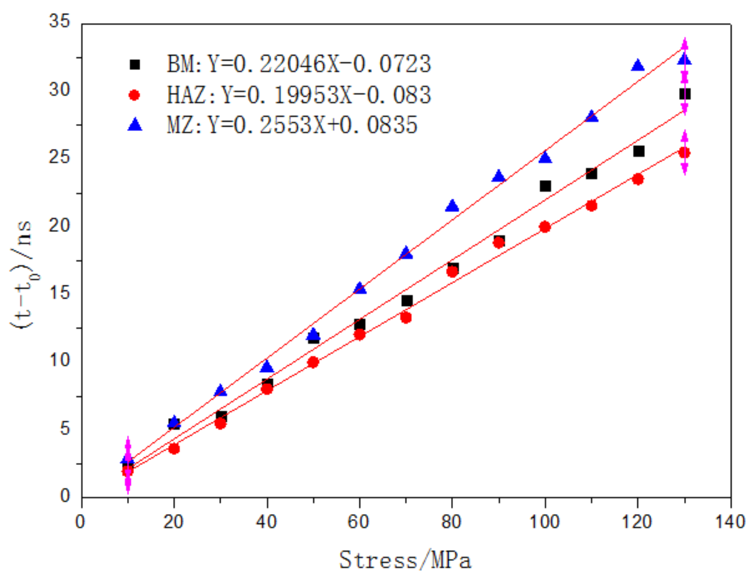

Fig. 7. (Color online) Result of tensile test to evaluate the K.

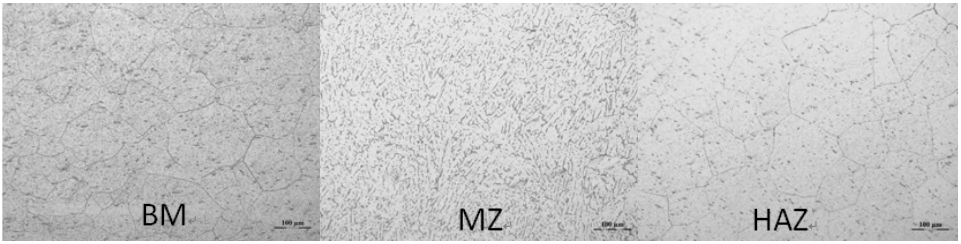

Fig. 8. Samples and microstructure in each zone.

were heat treated to reproduce the microstructure of the HAZ. The microstructure of different zones is shown in Fig. 8.

The calibration procedure was processed following the ASTM B557-10 standard. The Plexiglas wedge with fixing ultrasonic transducers was attached on the calibration samples. The direction of the L_{CR} wave transmission was parallel to the direction of residual stress measurement. The tensile samples were executed on the stretching machine DNS300. The results of tensile test are shown in Fig. 7 and also the K is 4.53, 5.1, and 3.91 for the BM, HAZ and MZ. In order to evaluate the residual stress according to Eq. (2), the value t_0 is measured directly from the stress-free sample that is created by employing the stress relieving heat treatment.

4. Residual and Discussion

In order to compare ultrasonic measurements and FE results, we need to verify that the FE models is accurate, iXRD model X-ray stress analyzer made by PROTO Corporation is used, and the measured point distributions are shown in Fig. 9.

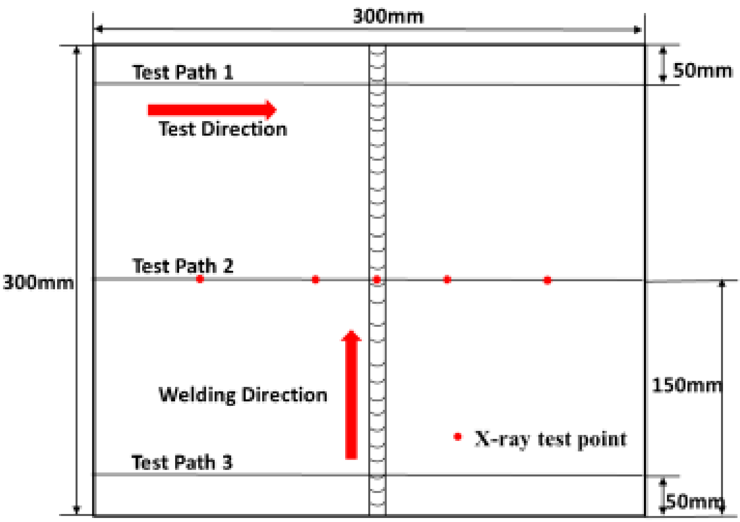

Fig. 9. (Color online) Path of distribution of LCR wave measurement and X-ray resting points.

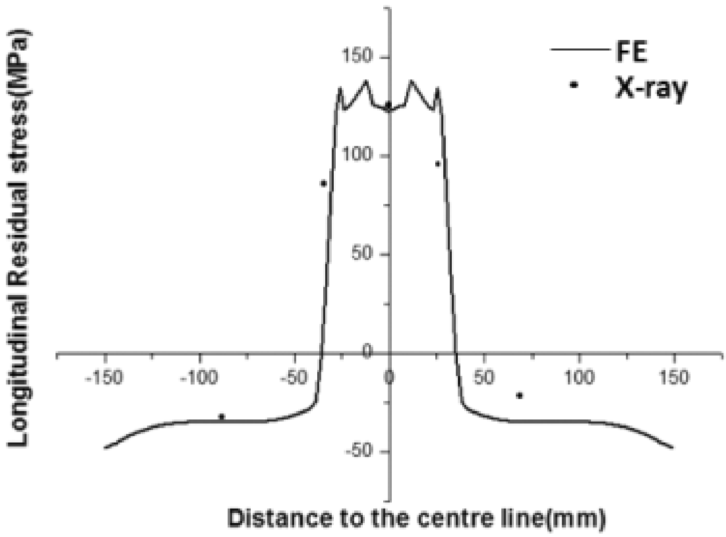

Fig. 10. The comparision of FE method and X-ray method according to residual stress.

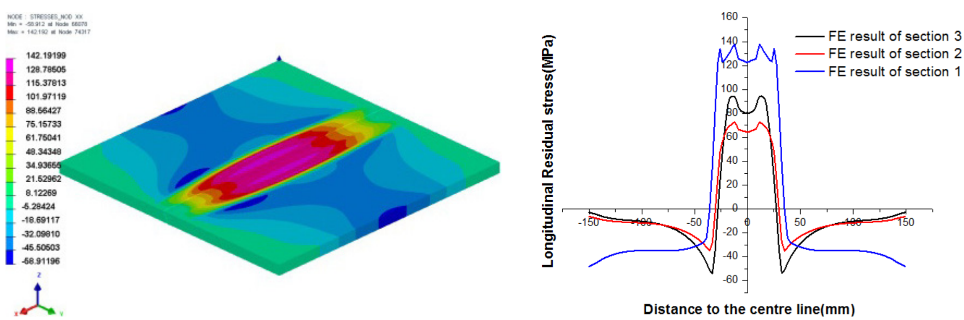

Fig. 11. (Color online) Longitudinal residual stress results of contour and three sections.

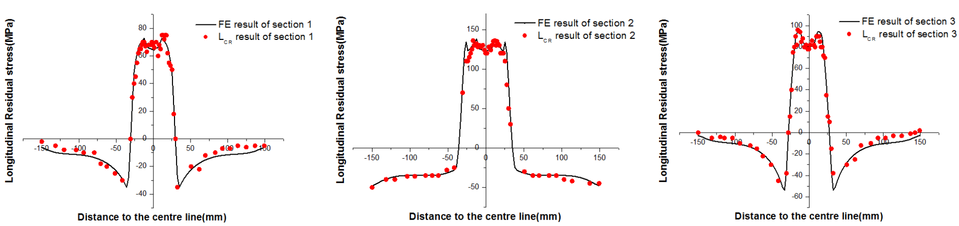

Fig. 12. (Color online) The compare of FE and LCR mothed of residual stress results in different testing path.

The longitudinal residual stresses analyzed by FE simulation are compared with those obtained from the X-ray measurements (Fig. 10) and a good agreement is achieved. This agreement can be considered as validation of FE welding simulation and proves the accuracy of FE model. Hence, the FE model could be employed in verifying the results of ultrasonic stress measurements.

The longitudinal residual stress results of contour and three sections that were obtained by the finite element method are shown in Fig. 11. These results are in good agreement with classical welding logic which says the maximum of tensile residual stress is produced in the weld centerline and it will be transformed to compressive stress near the HAZ and finally free stress zone in the parent material.

The results of ultrasonic measurements in different sections are shown in Fig. 12. All of the results of ultrasonic measurements are compared with finite element analysis showing an acceptable agreement. The maximum deviation of ultrasonic and FE results appears in the HAZ area because of the complicated microstructure of this region. The wave speed for LCR waves is affected by the average stress in a layer which may be a few millimeters thick, it means that stress measured by LCR approach represents the average value in a fixed path and may result in noticeable errors in residual stress sections with high gradients. In order to get a good result in the HAZ, a probe with higher spatial resolution needs to be used.

5. Conclusion

The present work shows that the longitudinal critically refracted waves can be used in the determination of the magnitude of the residual stress of 6082-T6 aluminum alloy, according to the achieved results, it can be concluded that:

(1) The microstructure in WZ, HAZ and BM zone have a significant effect on the K, especially in WZ, it is necessary to correct the errors resulted from different microstructure in order to avoid the overestimated residual stress.
(2) The finite element results are in good agreement with welding logic which says the maximum of tensile residual stress is produced in the weld centerline; it will be transformed to compressive stress near the HAZ and finally free stress zone in the parent material.
(3) The comparison between the residual stress calculated by SYSWELD and those obtained from the ultrasonic measurement shows a good agreement. It is demonstrated that the residual stress of 6082-T6 aluminum alloy welded plate can be evaluated by using the ultrasonic method.
(4) The maximum deviation of ultrasonic and FE results appears in the HAZ area because of the complicated microstructure of this region, how to improve the spatial resolution of L_{CR} method is an important problem.

Acknowledgment

The authors acknowledge the financial support from the National Key R&D Program (No. 2016YFB1200602-16).

References

1. K. Watanabe *et al.*, *IEEE Trans. Appl. Supercond.* **20**, 1420 (2010).
2. R. B. Gou *et al.*, *Insight Non-Destr. Test. Cond. Monit.* **57**, 556 (2015).
3. P. S. Prevey, *ASM Int. ASM Handbook* **10**, 380 (1986).
4. L. Meisner *et al.*, *Appl. Surf. Sci.* **280**, 398 (2013).
5. H. Palkowski *et al.*, *Materials* **6**, 5118 (2013).
6. M. H. Andrino *et al.*, ASME Pressue Vessels & Piping Conference **6**, 157 (2007).
7. A. A. Santos and D. E. Bray, *J. Press. Vessel. Technol.* **124**, 354 (2002).
8. Y. Javadi, M. Akhlaghi and M. A. Najafabadi, *Res. Nondestruct. Eval.* **25**, 30 (2014).
9. O. A. Godin, *J. Acoust. Soc. Am.* **125**, 117 (2009).
10. J. Goldak, *Matal. Trans. B* **15B**, 299 (1984).
11. D. M. Egle and D. E. Bray, *J. Acoust. Soc.* **60**, 741 (1976).